5 Discussion

This section discusses the cyclic and constant-load CGRs for the Davis-Besse CRDM nozzle Alloy 600 and J–groove weld Alloy 182, and for the V.C. Summer Alloy 182 butter and Alloy 82 weld alloys. It also addresses issues relating to the comparison of field and laboratory-prepared welds.

5.1 Alloy 600 from Davis-Besse CRDM Nozzle #3

The experimental CGRs under cyclic loading are compared in Fig. 67 with those predicted in air under the same loading conditions. Such plots allow direct comparison of cyclic CGR data obtained at different test temperatures, load ratios, and frequencies. Although the results show considerable scatter, environmental enhancement of growth rates is observed in all specimens of the Davis–Besse CRDM nozzle alloy. Also, specimen orientation does not seem to have any effect on growth rates, e.g., the CGRs for Specimens N3CL–1 and N3CC–3 are comparable, and those for Specimen N3CC–2 are slightly lower. For comparison purposes, the cyclic CGRs for Alloy 600 from the Davis–Besse CRDM Nozzle #3 in PWR water may be represented by the best–fit curve for Alloy 600 in normal water chemistry (NWC) for the BWR environment (i.e., Eq. 3 for Alloy 600 in ≈300 ppb DO at 289°C), although the environment is totally unrelated to that of interest. The experimental CGRs for Specimens N3CL–1 and N3CC–3 are slightly higher than the curve, and those for Specimen N3CC–2 are lower.

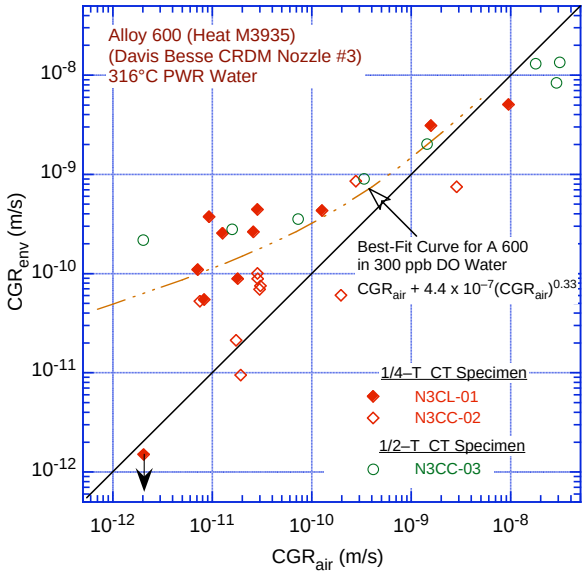

Figure 67.
CGR data for Davis–Besse CRDM Nozzle #3 Alloy 600 in PWR water at 316°C under cyclic loading.

The fatigue CGR data obtained earlier at ANL indicated that in low–DO water, environmental enhancement of CGRs in Alloy 600 seems to depend on material conditions such as yield strength and grain boundary coverage of carbides.[30] Materials with high yield stress and/or poor grain–boundary carbide coverage showed environmental enhancement. The results of the Davis–Besse CRDM Nozzle #3 Alloy 600 appear to be inconsistent with this trend, e.g., the nozzle #3 alloy has relatively low yield stress (Table 8) and appears to have good grain–boundary carbide coverage (Fig. 19). However, the loading conditions for the present tests are different from those for the earlier tests. In Alloy 600, environmental enhancement of CGRs is typically observed when load ratio R is ≥0.5, and rise time for the loading cycle is ≥30 s. For the earlier tests,[30] although the load ratios were in the range of 0.6–0.9, the rise time for all tests was only 12 s.

The fracture mode does not seem to influence the cyclic CGRs of the Davis–Besse CRDM Nozzle #3 Alloy 600. Although the fracture surface of N3CC–3 (Fig. 45) shows a larger fraction of TG fracture than that of N3CL–1 (Fig. 39), the CGRs for the two specimens are comparable.

The experimental CGRs under constant load, with or without partial unloading, are plotted as a function of applied K_{max} in Fig. 68a. The median and 75th percentile CGR curves based on the best fit of the data for 26 heats of Alloy 600 (Eq. 4) are also included in the figure. The CGR curves at 316°C were calculated using an activation energy of 130 kJ/mol. The growth rates for the Davis–Besse nozzle Alloy 600 are a factor of 4–8 higher than the median curve.

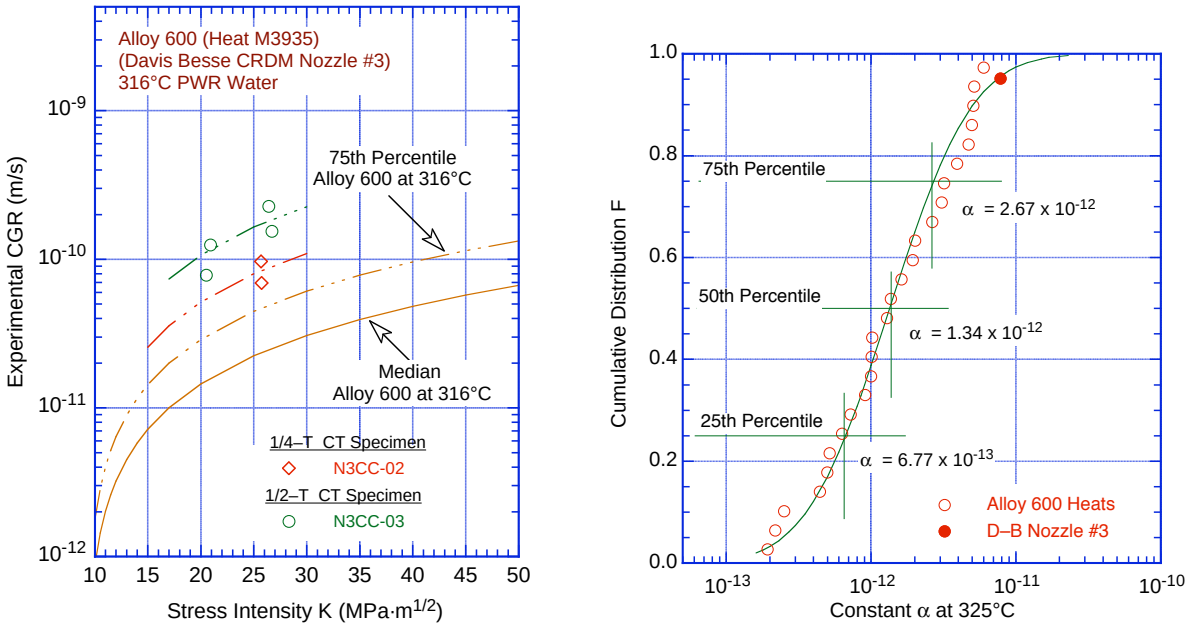

Figure 68. (a) CGR data for Davis–Besse CRDM Nozzle #3 Alloy 600 in PWR water at 316°C under constant load and (b) log–normal distribution of constant α for 26 heats of Alloy 600 [36].

The cumulative distribution of the log–normal fit to the ordered median ranking of the constant α for various data sets of Alloy 600 is shown in Fig. 68b. The experimental CGRs for Alloy 600 from Davis–Besse CRDM Nozzle #3 correspond to the ≈95 percentile of the distribution; i.e., the nozzle material exhibits very high susceptibility to SCC compared to other heats of Alloy 600.

5.2. Fatigue CGRs for Ni–alloy Weld Metals in Air

The database on fatigue CGR (da/dN) on Ni–alloy weld metals (e.g., Alloys 182, 82, 152, and 52) in air is very limited.[43–47] The database has results from ≈35 tests on Alloy 182 and 4 on Alloy 52; nearly 75% of the data are at room temperature and the remaining are at 320°C. An additional 94 tests on Alloys 82, 182, 52, and 152 weld metals in PWR water at low load ratios (e.g., ≤0.3) and/or high frequency (e.g., ≥0.1 Hz) may be included in the analysis because, under these loading conditions, CGRs are controlled primarily by mechanical fatigue. However, even these combined data on Ni–alloy weld metals are inadequate to establish the effects of stress ratio R, cyclic frequency, and stress intensity factor range ΔK on the CGRs. Consequently, the functional forms for effects of frequency, R, and ΔK in Eq. 1 were assumed to be the same as those for Alloy 600. The temperature dependence of constant C was

determined from data sets that were normalized for the effects of R and ΔK (Fig. 69). The CGR (m/cycle) of Ni–alloy welds, such as Alloys 82, 182, 52, and 152, in air may be expressed as

$$da/dN = C_{Niweld}\,(1 - 0.82\,R)^{-2.2}\,(\Delta K)^{4.1}, \tag{14}$$

where ΔK is in MPa·m$^{1/2}$, and C_{Niweld} is given by a fourth-order polynomial of temperature T(°C), expressed as

$$C_{Niweld} = 8.659 \times 10^{-14} - (5.272 \times 10^{-17})T + (2.129 \times 10^{-18})T^2 - (1.965 \times 10^{-20})T^3 + (6.038 \times 10^{-23})T^4. \tag{15}$$

The predicted–vs.–experimental CGRs for Ni–alloy weld metals at various temperatures in air and PWR environment under predominantly mechanical fatigue loading conditions are shown in Fig. 70. The predicted values show good agreement with the experimental results. Under similar loading conditions, the fatigue CGRs of Ni–alloy welds in air are a factor of 2–3 higher than those of Alloy 600.

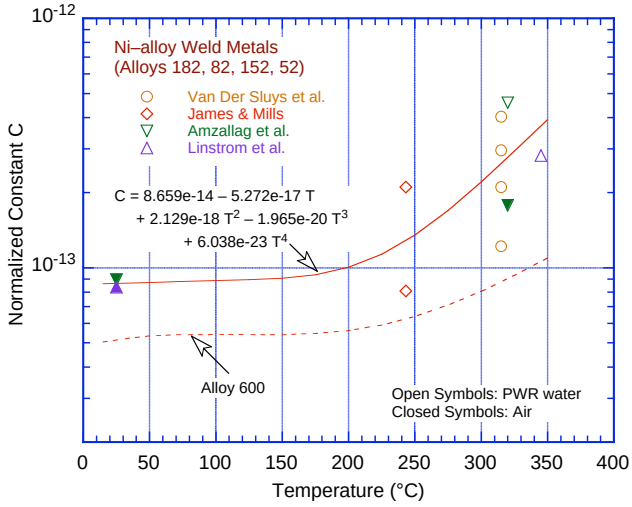

Figure 69.
Variation of normalized constant C for Ni–alloy weld metals with temperature.

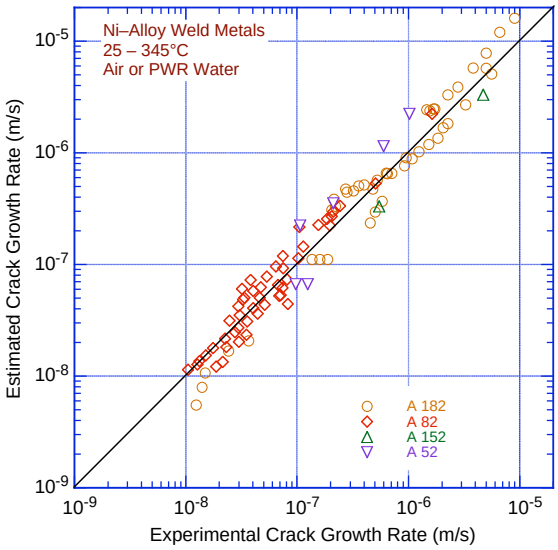

Figure 70.
Predicted–vs.–experimental values of fatigue CGR of Ni–alloy weld metals in air and PWR environment under predominantly mechanical fatigue loading conditions.

Figure 71 shows the experimental-vs.–predicted values of fatigue CGR of Alloys 182 (Fig. 71a) and 82 (Fig. 71b) in air and in a PWR environment.[43–47] Although not all of the data were used for determining Eq. 15, both data sets are in good agreement with the predicted values. Limited data are available for Alloys 182 and 82 for high R and low frequencies. They indicate that the enhancement due to the PWR environment is modest. The data for Alloy 182 for $CGR_{air} < 10^{-9}$ m/s where environmental enhancement might be expected to be increasing is very limited. However, the Alloy 82 data suggest that effects may be relatively small and that the cyclic CGRs of Ni–alloy welds in PWR water may either be bounded by $5 \times CGR_{air}$ or may be represented by the expression

$$CGR_{env} = CGR_{air} + 0.018\,(CGR_{air})^{0.78}. \quad (16)$$

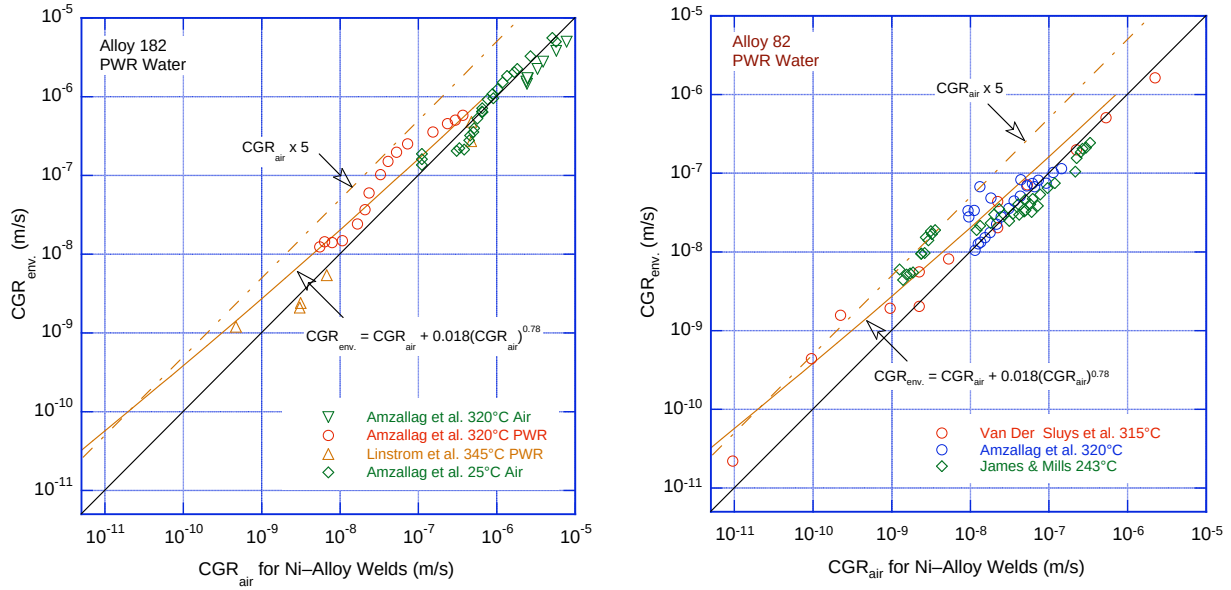

(a) (b)

Figure 71. Experimental-vs.–predicted values of fatigue CGR of (a) Alloy 182 and (b) Alloy 82 in air and in a PWR environment [Refs. 42–46].

5.3 Ni–Alloy Welds

5.3.1 From Davis–Besse CRDM Nozzle #11

The experimental CGRs for Alloy 182 weld specimens from the Nozzle #11 J–groove under cyclic loading and those predicted for Ni-alloy welds in air under the same loading conditions are shown in Fig. 72a. The cyclic CGRs for the 1/2–T CT specimen show some environmental enhancement whereas those for the 1/4–T CT specimen show little or no enhancement. The cyclic CGRs for Alloy 182 from the D–B CRDM Nozzle #11 J–groove weld may be represented by Eq. 16. The CGRs obtained under constant load (with or without periodic partial unloading) are shown in Fig. 72b. Under constant load, the CGRs for the 1/2–T CT specimen are slightly higher than those for the 1/4–T CT specimen. However, in a PWR environment, the growth rates for the Davis–Besse J–groove weld alloy are an order of magnitude lower than the proposed disposition curve for Alloy 182 welds.[37] Figure 74b shows that the measured CGRs correspond to about the 20th percentile for the population of Alloy 182 welds.

The root cause for the low SCC growth rates is not clear. However, several out–of–plane cracks are observed along the crack front (Fig. 50). These cracks may be preexisting (e.g., hot cracks) or may

have formed during the tests (e.g., crack branching at the crack tip). These out–of–plane cracks appear to impede crack advance and may be responsible for the low CGRs in the material.

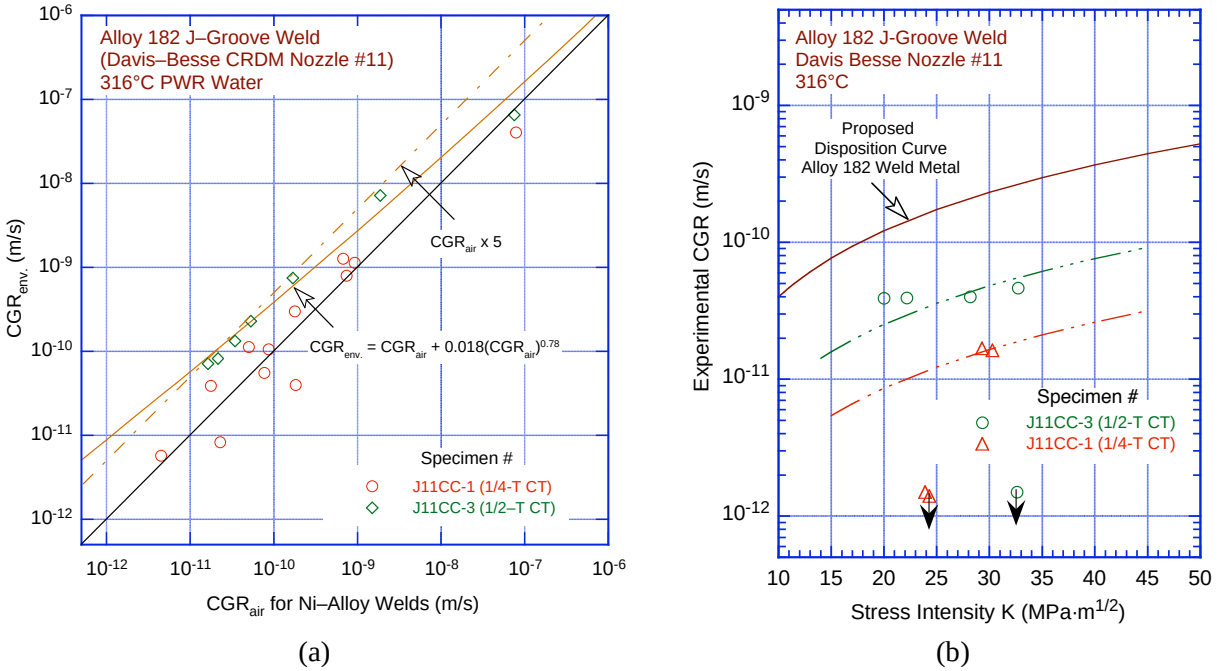

Figure 72. Cyclic CGR data for Alloy 182 from the Davis–Besse CRDM Nozzle #11 J–groove weld in a PWR environment at 316°C under (a) cyclic loading and (b) constant load.

5.3.2 From V.C. Summer Reactor Vessel Nozzle–to–Pipe Weld

Figure 73 shows the CGR rates under cyclic loading for the three V.C. Summer Ni-alloy weld specimens, WCR–01, BCR–01, and WLR–01, as a function of the CGRs predicted for Ni-weld alloy in air under the same loading conditions. When environmental enhancement occurs, the relative CGRs in the PWR environment compared with those in air should be increasing with decreasing CGRs in air. The results indicate that under predominantly mechanical fatigue loading conditions (i.e., low load ratios and high frequency), the CGRs for the V.C. Summer weld alloys are a factor of ≈5 lower than those typically observed for laboratory–prepared Alloy 182 or 82 welds. The growth rates for the weld alloys are even lower than the rates typically observed in Alloy 600. Some environmental enhancement of CGRs is observed under loading conditions that result in CGRs less than 1×10^{-9} m/s in air (i.e., load ratios ≥0.5 and rise times ≥30 s), particularly for Specimen WLR–01 (shown as open diamonds in Fig. 73). These conditions also result in a change in fracture morphology (e.g., from TG to predominantly IG fracture).

The results also indicate that the alloy type (Alloy 82 weld or Alloy 182 butter material) or the weld structure (specimen orientation) has little or no effect on the fatigue CGRs of these materials. For example, the CGRs of the Alloy 82 weld material (Specimens WLR–01 and WCR–01) are comparable to those of the Alloy 182 butter material (Specimen BCR–01). Also, in Specimens WLR-01 and WCR-01, although the crack growth direction is along the dendrites whereas in Specimen BCR–01 it is across the dendrites, the CGRs under similar environmental and loading conditions are comparable for all specimens. These results are consistent with the existing fatigue CGR data for Ni–alloy welds in a PWR environment. [43–47]

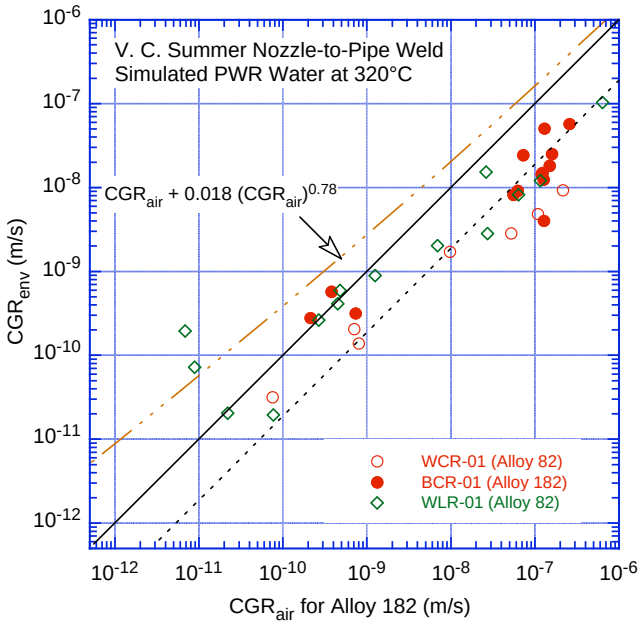

Figure 73.
Fatigue CGR data for V.C. Summer Ni–alloy welds in a PWR environment plotted as a function of the growth rate for Ni-alloy welds in air under the same loading conditions.

Figure 74a shows CGR data under constant load for the V.C. Summer weld alloys. Results from Jacko et al.[53], on the same alloys, are also included in the figure. The CGR for Specimen WLR-01 at K_{max} = 31.2 MPa·m$^{1/2}$ (period 5, Table 17) was considered anomalous, and thus not included in Fig. 74a. The CGRs of Alloy 82 weld material (Specimens WLR–01 and WCR–01) with growth direction along the dendrites are comparable to those of the Alloy 182 butter material (Specimen BCR–01) with growth

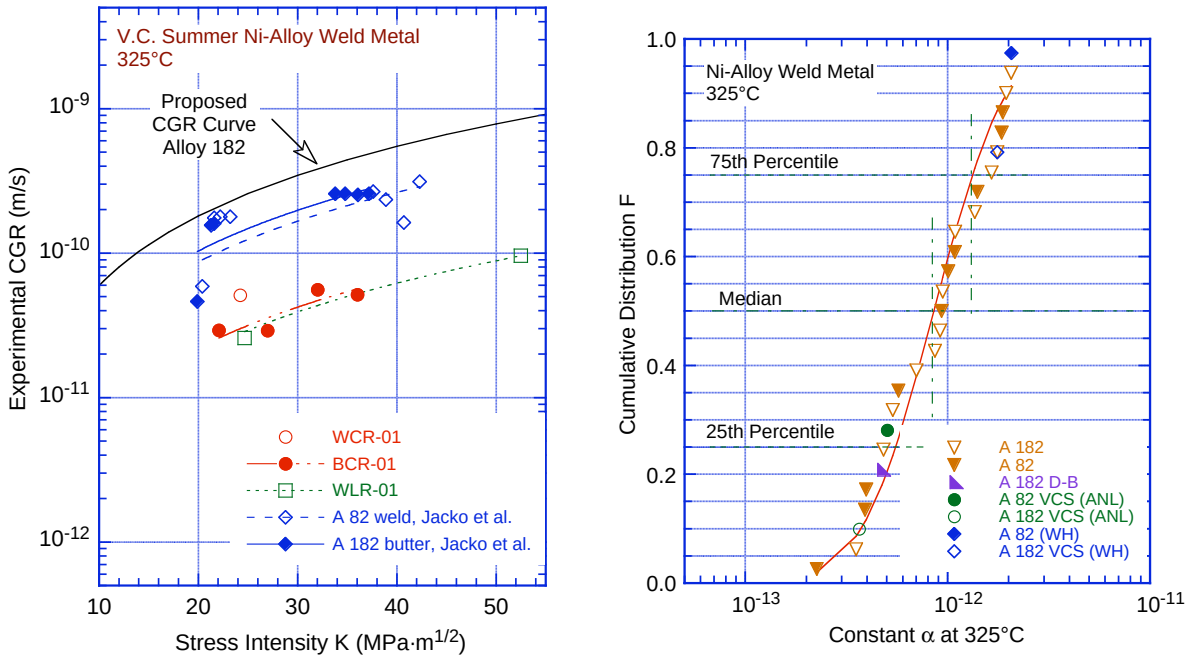

Figure 74. (a) CGR data for Alloy 182 and 82 nozzle-to-pipe butter and weld specimens from V.C. Summer in PWR environment at 325°C under constant load and (b) log–normal distribution of constant α for several heats of Alloys 82 and 182.

direction transverse to the dendrites. In general, CGRs in Alloy 182 are a factor of 2.5 higher than in Alloy 82; however, the rates along a direction transverse to the dendrites are a factor of ≈2 lower than those parallel to the dendrites. The effects of alloy type and specimen orientation seem to have cancelled each other, yielding approximately the same growth rates for the weld and butter alloys. However, the CGRs from the present study are a factor of ≈4 lower than those obtained by Jacko et al.[53] Also, the CGRs for the V.C. Summer alloys from the present study are comparable to those determined for the Davis–Besse CRDM nozzle J–groove weld.

Figure 74b shows the cumulative distribution of the log–normal fit to the ordered median ranking of the constant α in Eq. 5 for various data sets of Ni-base weld alloys available in the literature. It essentially is a ranking of the various heats with respect to their susceptibility to SCC. The results of Jacko et al.[53] suggest that the V.C. Summer weld and butter alloys correspond to the ≈95 and 80 percentile, respectively, of the distribution of the various heats, whereas, the results from the present study indicate that they correspond to the ≈25 and 10 percentile, respectively. The reasons for the differences in the results between the two studies is not clear. The crack fronts in the tests reported here are relatively straight. The crack fronts in the tests in Jacko et al.[53] do not appear to be as straight. CGRs in isolated "fingers" may be more rapid than the overall growth of a straight crack front.

5.4 Variability in Ni-Alloy CGR Data

The Alloy 600 material from Davis-Besse Nozzle #3 (Heat M3935) is highly susceptible to SCC and ranks at the estimated 95th percentile of heats of Alloy 600 that have been investigated to develop the CGR disposition curve for this alloy in PWR environments. The proposed disposition curve is based on the 75th percentile of the CGR distribution for the available heats; the data for the Davis–Besse CRDM Nozzle #3 alloy is above the disposition curve. The reasons for the high growth rates for this alloy are still unclear.

On the basis of the observed microstructure and tensile strength of the Davis–Besse CRDM nozzle Alloy 600, the experimental CGRs are somewhat of a surprise. Materials with a good GBC of carbides (Fig. 19) and relatively low or average tensile yield stress (Table 8) are generally considered to have low susceptibility to SCC in PWR water.[48–57] The high susceptibility of the material to SCC cannot is inconsistent with expectations based on the tensile strength and microstructure of the alloy.

The most striking result for the Davis–Besse nozzle Alloy 600 is that the cracking mode was IG from the start in two of the three samples tested. The finding that IG growth takes place in a regime dominated by mechanical fatigue (which would be expected to result in a TG growth) suggests that the grain boundaries have undergone some form of sensitization during fabrication and/or the two decades of service. The fact that not all three specimens exhibited IG fracture from the beginning suggests that some regions in the nozzle may be more susceptible than others.

The composition of the Davis–Besse nozzle alloy is within ASTM specifications. It is also for the most part within the range of compositions of the heats that have been used to develop the CGR disposition curve for thick–section Alloy 600 in PWR environments.[36] The only exception is the rather low Fe content in the Davis–Besse nozzle alloy, e.g., 5.93 wt.% in the nozzle alloy compared with the range of 7.0–9.5 wt.% for the heats used to develop the disposition curve. The significance of the low Fe content on SCC susceptibility of the alloy is not clear.

Metallographic examination of the alloy did not indicate any unusual features that would explain the relatively high growth rates in this alloy. Although Ti–rich precipitates were observed in the material,

they do not seem to affect the fracture behavior (Fig. 43c). The precipitation of Ti carbides can reduce the concentration of free carbon in the matrix to a level at which it may limit the formation of the desirable grain–boundary chromium carbides. However, the Davis–Besse nozzle Alloy 600 shows good GBC of carbides. It also has a significant amount of intragranular carbides. An earlier detailed microstructural characterization of Ni–alloys by conventional metallographic and analytical electron microscopy techniques[58] indicated that materials that appear to be similar by optical metallographic analysis can exhibit pronounced microstructural differences in terms of the extent and nature of carbide precipitation. The materials most resistant to SCC were found to contain continuous or semicontinuous intergranular Cr–rich M_7C_3 carbides with a dendritic morphology and little or no distribution of intragranular carbides. A more detailed microstructural characterization of the Davis–Besse CRDM nozzle alloy may provide helpful information in understanding the susceptibility of these alloys to PWSCC.

The Alloy 182 or 82 materials from the Davis–Besse CRDM nozzle J–groove weld or the V.C. Summer reactor vessel nozzle–to–pipe weld and butter appear to be quite resistant to cracking compared to the available data. The proposed disposition curves for Ni–alloy welds, which are based on the 75th percentile of the CGR distribution for the available heats, are conservative for the weld alloys from the V.C. Summer and Davis–Besse reactors. This is true even for the CGRs determined by Jacko et al.[53]

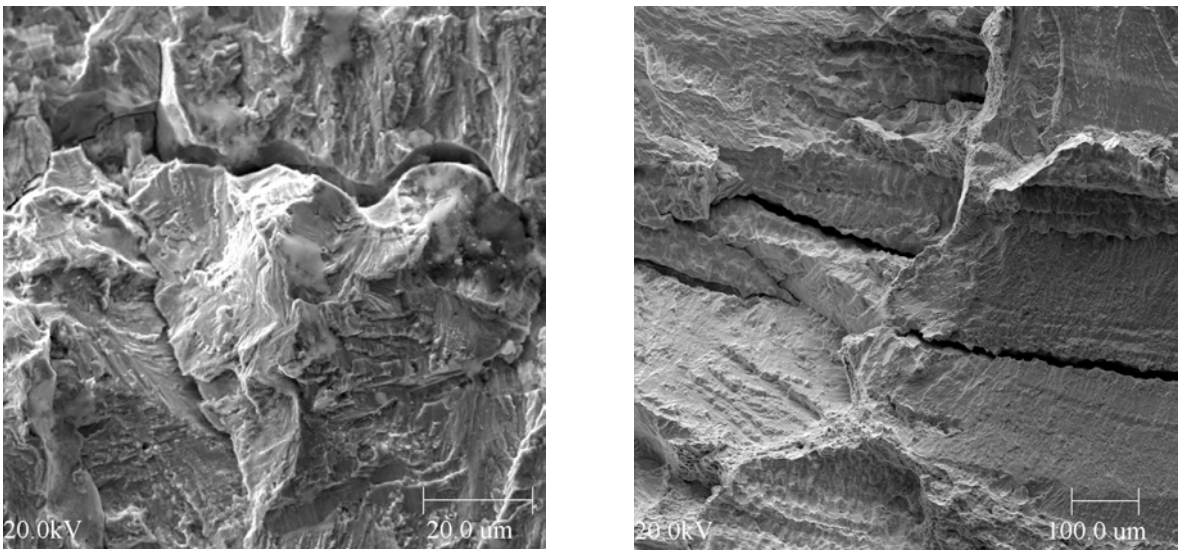

(a) (b)

Figure 75. Micrographs from the fracture surface of weld specimens: (a) Davis-Besse Specimen J11CC–1 and (b) V.C. Summer Specimen BCR–01.

The appearance of the fracture surfaces of the weld alloys suggests that pinning by defects and precipitates could play a role by impeding crack propagation. In addition to the "pinned" fracture surfaces, another common feature observed in all specimens, with the exception of one of the V.C. Summer specimens, is the cracks on the fracture surface parallel to the crack front and transverse to the crack plane, where the propagating SCC cracks seem to arrest. Micrographs are shown from Davis-Besse Specimen J11CC-1 (Fig. 75a) and V.C. Summer Specimen BCR–01 (Fig. 75b). The only specimen that did not exhibit such cracks was WCR-01 (see, for example, Fig. 58), and this specimen had the highest measured CGR of all weld specimens. At present, it is not clear whether these are preexisting cracks (e.g., hot cracks) or whether they were formed during the tests (e.g., by crack branching at the crack tip). In any case, these out–of–plane cracks appear to impede crack advance and may be responsible for the low CGRs in the material.